

Nonstandard top substructureChristoph Englert,^{1,*} Dorival Gonçalves,^{2,†} and Michael Spannowsky^{2,‡}¹*SUPA, School of Physics and Astronomy, University of Glasgow, Glasgow G12 8QQ, United Kingdom*²*Institute for Particle Physics Phenomenology, Department of Physics, Durham University, Durham DH1 3LE, United Kingdom*

(Received 22 January 2014; published 21 April 2014)

The top quark, being the heaviest particle of the Standard Model (SM), is a prime candidate of where physics beyond the SM (BSM) might currently hide before our eyes. There are many natural extensions of the SM that rely on top compositeness, and the top quark could follow the paradigm of revealing a substructure when it is probed at high enough momentum transfers. Observing high p_T top final states naturally drives us toward boosted hadronic analyses that can be tackled efficiently with jet substructure techniques. In this paper we analyze the prospects of constraining exemplary nonstandard QCD top interactions in this kinematical regime. We correctly include QCD modifications to additional gluon emission off the boosted top quark and keep track of the modified top tagging efficiencies. We conclude that nonstandard top QCD interactions can be formidably constrained at the LHC 14 TeV. Experimental systematic uncertainties are a major obstacle of the described measurement. Unless significantly improved for the 14 TeV run, they will saturate the direct sensitivity to nonresonant BSM top physics at luminosities of around 100/fb.

DOI: 10.1103/PhysRevD.89.074038

PACS numbers: 14.65.Ha, 12.60.-i, 12.38.-t

I. INTRODUCTION

After the discovery of a Standard Model (SM) Higgs boson [1] at the LHC [2,3] and preliminary measurements of its properties and couplings [4,5] which indicate close resemblance to the SM hypothesis, hints for physics beyond the SM (BSM) remain elusive. A puzzle that remains in the context of SM irrespective of a seemingly unnatural electroweak scale is the mass hierarchy in the fermion sector and the large mass of the top quark rather close to the Higgs vacuum expectation value. The restoration of chiral symmetry for vanishing Yukawa interactions guarantees that corrections to elementary fermion masses are proportional to the fermion masses themselves in the SM. Using the language of effective field theory, the Yukawa couplings are marginal operators; i.e. once their values are fixed by some UV dynamics [6], they remain small at low energy scales. Hence, the large hierarchy among the Yukawa couplings largely determined by the top quark is typically considered a potential source of physics beyond the SM.

Indeed, the top typically plays a central role in most models that try to explain the electroweak scale at a more fundamental level. Supersymmetric constructions [7], fixed-point gravity scenarios [8], and strong interactions [9] are just three well-known and well-established examples. In the latter case, the large mass of the top can be understood as a (linear) mixing effect of light elementary

states with composite fermions of a strongly interacting sector [10–12] that also provides a set of Nambu Goldstone bosons forming the Higgs doublet. The mixing effects together with fermion and gauge boson loops induce a Coleman-Weinberg Higgs potential that triggers breaking of electroweak symmetry at a scale much smaller than the strong interaction scale. In such pseudo-Nambu Goldstone Higgs scenarios, we can have a large resemblance of the Higgs phenomenology with the SM, while the composite effects are hidden in the fermionic sector. Phenomenological searches that target the potential substructure of the top quark are therefore also extremely important in the context of Higgs physics, since both phenomena, the $\mathcal{O}(100\text{ GeV})$ electroweak scale with the top quark in the same ball park, might point us toward a solution in terms of strong interactions.¹

Of course, the phenomenological implications of compositeness are not new to particle and, more broadly speaking, to nuclear physics (see Ref. [14] for a review). The deviation from the anticipated Rutherford scattering cross section at large angles observed by Geiger and Marsden [15] and the later resolution of atomic nuclei [16,17] is a well-known example of such a program resolving pointlike sources by probing the characteristic energy scale with high enough momentum transfers. The nonlinear structure of QCD and the mismatch of the theory's fundamental degrees of freedom with the experimental observables, however, introduce

*christoph.englert@glasgow.ac.uk

†dorival.goncalves@durham.ac.uk

‡michael.spannowsky@durham.ac.uk

¹It should be noted that such interactions typically also alter low energy observables (see, e.g., Ref. [13]), but we remind the reader that we focus on the prospects of *direct* measurements in this work.

another layer of complexity when we deal with nonstandard interactions of a color-charged object. We usually parametrize the deviations from the SM via introducing higher dimensional operators in an effective field theory description that is guided by the low-energy gauge symmetry requirements. Since we can expect a separation between the new physics and the electroweak scale, it is customary to limit analyses to dimension six operator extensions to the SM [18–21]. However, since we cannot separate different partonic initial and final states and due to the gauge structure, all operators that introduce nonstandard QCD properties will contribute simultaneously. Their different kinematical dependencies can be used to disentangle them [22,24–26], but modifications due to new interactions will also change the response of the measurement strategy.

The top quark production cross section will receive modifications for energetic events if new physics in the top sector is present. This immediately motivates boosted top searches [27] as a sensitive probe of modified QCD interactions on which we focus our analysis in the following. From previous analyses [26] it is expected that upon correlating inclusive and boosted measurements of $pp \rightarrow t\bar{t} + X$ we will be able to tightly constrain such nonstandard interactions. However, there is a caveat: top quarks when produced at high p_T are very likely to emit hard gluons before they decay [28,29]. In Ref. [26] it was shown that such an interaction has a decreased sensitivity to anomalous QCD top interactions. It is therefore crucial to include the anomalous top interactions to the proper modeling of the exclusive final state to correctly evaluate the prospects of the described measurement. By analyzing the fully hadronized final state in such a setup, we are also guaranteed to correctly reflect the different selection efficiencies for the boosted subject analysis that emerge from the BSM-induced modifications of the top spectrum. More precisely, we investigate the constraints that we can expect from adapted searches for anomalous top interactions in the busy QCD-dominated LHC environment using realistic simulation, analysis and limit setting techniques.

Especially experimental systematics are known to be large in the tails of top distributions where the deviations from the SM will be most pronounced. Unless these uncertainties are properly included in the formulation of the BSM limits, we cannot trust the analysis. We discuss the present systematics and include them in our CLs [30] projection for the 14 TeV LHC run in the most conservative way. To keep our analysis transparent we focus on two representative anomalous top-QCD operators that are characteristic for composite fermionic structures from a QCD point of view, namely color charge radius and anomalous magnetic moment [31] (see Ref. [32] for similar work on composite leptons). The generalization to other nonstandard top-related interactions is straightforward.

II. A PHENOMENOLOGICAL APPROACH TO ANOMALOUS QCD TOP INTERACTIONS

To get a quantitative estimate of the leading effects of nonstandard top interactions at the LHC we focus on new physics contributions to $t\bar{t}$ production arising from modified QCD interactions. Nonstandard electroweak properties do impact the top decay $t \rightarrow Wb$ [33], but can be studied separately in single top production and interlaced with our findings.

Since the current LHC searches imply strong bounds on the masses of potential new degrees of freedom, it is expected to have a mass gap between the SM and the BSM fields (which, e.g., lift the top mass via mixing effects [34]). In this case, the new physics effects can be parametrized via higher dimension operators involving only the SM particles, and there is a number of new contact operators which impact $t\bar{t}$ + jets production [20,22]. Here we focus on some operators that allow an interpretation in terms of composite structures such as radii and anomalous magnetic dipole moments as a proof of principle. These nonstandard properties can be introduced in a gauge-covariant way through the following effective dimension six interaction terms² [19,24–26]:

$$\mathcal{L}_R = -g_s \frac{R_t^2}{6} \bar{t} \gamma^\mu G_{\mu\nu} D^\nu t + \text{H.c.}, \quad (1a)$$

$$\mathcal{L}_k = g_s \frac{1}{4m_t} \bar{t} \sigma^{\mu\nu} (k_V + ik_A \gamma^5) G_{\mu\nu} t, \quad (1b)$$

where G_μ is the gluon field, $G_{\mu\nu} = D_\nu G_\mu - D_\mu G_\nu$ its field strength and $D^\mu = \partial^\mu + ig_s G^\mu$ the covariant derivative. The convention of Eq. (1) follows Ref. [32]; the top quark radius R_t and the anomalous chromomagnetic and chromoelectric dipole k_V, k_A moments are related to the new physics scale Λ in the “traditional” dimension six extension approach by³

$$R_t = \frac{\sqrt{6}}{\Lambda}, \quad k_{V(A)} = \rho_{V(A)} \frac{m_t^2}{\Lambda^2}, \quad (2)$$

where $\rho_{V(A)}$ is a $\mathcal{O}(1)$ parameter.

To have a consistent treatment of the dimension six operator expansion the new physics contributions are manifest only through the interference of these new physics

²It is worth mentioning that the top quark radius operator can be rewritten as a sum of four-fermion operators involving a pair of top and antitop in association with a pair of light quark and antiquark [22,23].

³Since we are interested in the interpretation of these new physics operators in terms of composite structures, the top radius coefficient is naturally positive. However, the values of k_V, k_A in principle could be negative, but in the present study for simplicity we assume that it is positive throughout the analysis. We will, however, comment on negative values at the end of the analysis section.

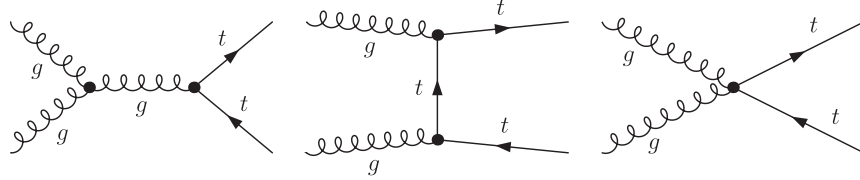


FIG. 1. Feynman diagrams contributing to anomalous $p(g)p(g) \rightarrow t\bar{t}$ production at leading order, arising from the operators of Eq. (1).

operators' contribution with the SM amplitude; i.e. we do not include terms to the hadronic cross section other than the ones that formally scale as $\mathcal{O}(1/\Lambda^2)$. Splitting the amplitude that results from Eqs. (1) into a SM and BSM piece

$$\mathcal{M} = \mathcal{M}_{\text{SM}} + \mathcal{M}_{\text{BSM}}(\Lambda^{-2}), \quad (3)$$

we have for the (partonic) cross section

$$\sigma \sim |\mathcal{M}_{\text{SM}}|^2 + 2\Re\{\mathcal{M}_{\text{SM}}\mathcal{M}_{\text{BSM}}^*(\Lambda^{-2})\} + \mathcal{O}(\Lambda^{-4}). \quad (4)$$

The expansion of the cross section to $\mathcal{O}(1/\Lambda^2)$ removes the chromoelectric operator from the $t\bar{t}$ sample [24] and the sensitivity to k_A arises from the less dominant $t\bar{t}j$ contribution. The squared BSM matrix elements has a dependence on k_A [24]. At $\mathcal{O}(1/\Lambda^4)$, however, when k_A becomes resolvable, we can also expect additional dimension eight operators to enter the stage via interference with the SM amplitude. In such a case it is not clear how to interpret a limit obtained on k_A . Expanding of the cross section to $\mathcal{O}(1/\Lambda^2)$ will therefore yield only mild constraints on k_A .

The deviations $\Delta\sigma$ from the SM Born-level partonic $t\bar{t}$ cross sections σ_B sketched in Eq. (4) factorize [22,24,26] as follows:

$$\frac{\Delta\sigma}{\sigma_B}(q\bar{q} \rightarrow t\bar{t}) = \frac{s}{3}R_t^2 + \frac{6k_V}{3-\beta^2}, \quad (5a)$$

$$\begin{aligned} \frac{\Delta\sigma}{\sigma_B}(gg \rightarrow t\bar{t}) \\ = \frac{k_V(36\beta - 64\tanh^{-1}\beta)}{\beta(59 - 31\beta^2) - 2(33 - 18\beta^2 + \beta^4)\tanh^{-1}\beta}, \end{aligned} \quad (5b)$$

where s is the squared partonic center of mass energy and $\beta = \sqrt{1 - 4m_t^2/s}$. Notice that for $q\bar{q}$ initial states both new physics contributions R_t and k_V are present, whereas for gg -induced production (the main production mode for inclusive $t\bar{t}$ production at the LHC) there is only sensitivity to the anomalous chromomagnetic moment k_V . This is due to gauge invariance of the dimension six operator; i.e., there is a Ward identity that guarantees the cancellation of the R_t

dependence⁴ in the sum of Fig. 1. It can be shown that for the $t\bar{t}j$ sample the same conclusion holds; i.e., the gg subchannel still has no dependence on the R_t parameter which originates from the $q\bar{q}$ and gq induced subprocesses [26].

We can enhance the fraction of the $q\bar{q}$ initial state and still probe R_t at the LHC by requiring boosted top events.⁵ This is because energetic events probe the incoming partons at high momentum fractions where the proton's valence quarks' parton densities peak. We illustrate this in Fig. 2, where we present the fractional contribution of each partonic subprocess to the hadronic SM $t\bar{t}(j)$ cross section as a function of the reconstructed $t\bar{t}$ mass and the top transverse momentum $p_{T,t}$. We can invoke cuts on either observable to suppress the gg initial state although $p_{T,t}$ is more effective and the more crucial observable in the context of top tagging [35,36].

III. DETAILS, ANALYSIS AND RESULTS

In our analysis we focus $t\bar{t}$ production with one top decaying semileptonically and the other hadronically. As this process involves the production of heavy colored particles and we are selecting the boosted kinematical regime, we can expect an important contribution from initial and final state jet radiation [37,38]. To take this sufficiently into account we include the BSM-mediated hard radiation effects via jet merging, keeping the full BSM dependence on the nonstandard parameters of the respective samples to $\mathcal{O}(\Lambda^{-2})$. As already mentioned, the dependencies on the top radius arise entirely from the $q\bar{q}$ and gq initial states. Therefore, to constrain this operator it is necessary to suppress the dominant subchannel at the LHC, namely the gg initial state. The boosted high p_T selection serves two purposes in this sense: it removes the less sensitive initial states and focuses on regions where deviations from the SM are large, Eq. (5).⁶

Our implementation starts by including the new interactions presented in Eqs. (1) through FEYNRULES [41],

⁴An identical cancellation is required to ensure a massless gluon in the extended theory: by closing the top loop we have a contribution to the gluon two-point function from the two diagrams on the right hand side of Fig. 1 which do not vanish in dimensional regularization.

⁵A similar strategy has been discussed in the context of the central-forward top asymmetry [35].

⁶It is worth noticing that for boosted final states we do not need to worry about trigger issues [39,40].

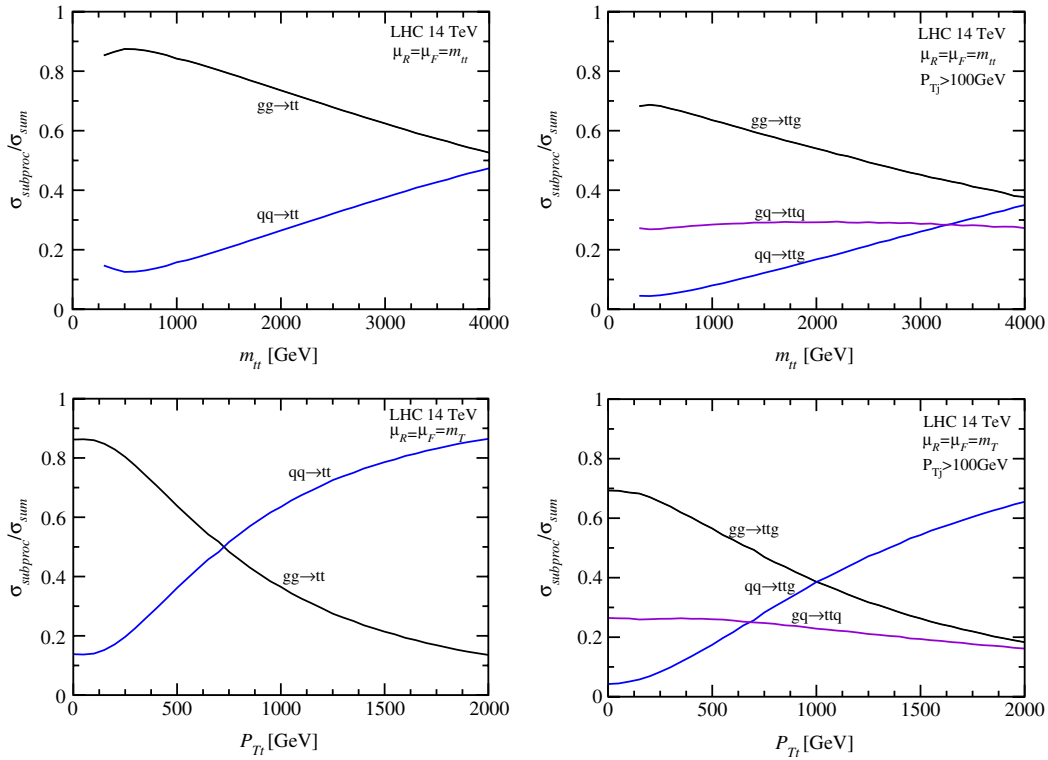


FIG. 2 (color online). Fractional contribution of each partonic channel to the hadronic cross section for $\sigma_{t\bar{t}}$ (left) and $\sigma_{t\bar{t}j}$ (right) production as a function of the cut on the reconstructed top pair mass $m_{t\bar{t}}$ (top) and the transverse momentum of the top $p_{T,t}$ (bottom). The born cross sections are generated for the LHC at $\sqrt{s} = 14$ TeV with the scales set at the reconstructed top pair mass $m_{t\bar{t}}$ (top) and the transverse mass m_T (bottom).

which outputs a UFO model file [42] that is further used in MADGRAPH5 [43]. MADGRAPH performs the event generation that is subsequently showered with PYTHIA6 [44] where we take into account the initial and final state radiation, hadronization and underlying event. The hard matrix elements have been adapted to include only the interference of the new physics amplitude with the SM counterpart; this way we guarantee a consistent expansion of the cross section up to $\mathcal{O}(\Lambda^{-2})$ as discussed earlier when the QCD emission is hard and sensitive to the BSM effects. We have validated our parton level matrix element implementation against existing analytic calculations as well as an independent Monte Carlo implementation [22,24,26].

The jet merging is subsequently performed by employing the MLM scheme [45] as implemented in the MADGRAPH package. Throughout the analysis we consider the LHC running at $\sqrt{s} = 14$ TeV, and the SM $t\bar{t}$ cross section normalization is rescaled to the next-to-next-to-leading order (NNLO) value, $\sigma_{\text{NNLO}} = 918$ pb [46]. We find that for our boosted selection that the background is completely dominated by SM $t\bar{t}$ production. All other background contributions are negligible and well below the SM $t\bar{t}$ uncertainty.

We include the expected dominant NLO shape modifications via aMC@NLO [47]: we construct a reweighting function with respect to the $R_t, k_V, k_A = 0$ sample (the SM)

to account for differential QCD corrections in the BSM histograms. This is a necessary procedure to have a well-defined limit $R_t, k_V, k_A \rightarrow 0$. Throughout, we choose the renormalization and factorization scales as the transverse mass since this choice yields a rather flat scale dependence of the NLO matched $t\bar{t}$ cross section, Fig. 3.

Instead of proceeding as in a “traditional” semileptonic $t\bar{t}$ analysis we take advantage of the efficient top tagging for high p_T fat jets. This is facilitated by defining a fat jet with a large cone size $R = 1.5$ using the Cambridge/Aachen algorithm as implemented in FASTJET [48]. We require at least one of these objects to have a transverse momentum larger than $p_{T,\text{fatjet}} > 600$ GeV. We choose this exemplary value due to a large top tagging efficiency $\sim 30\%$ and a small fake rate $\sim 3\%$.⁷ For this threshold the $t\bar{t}$ cross section

⁷The nonstandard QCD-top interactions imply a subdominant effect on the top tagging efficiency of $\mathcal{O}(1\%)$. Only in two ways could these interactions change the tagging efficiency of the top quark: either by changing the p_T of the top or by inducing more radiation in the event. Since we show the differential cross section with respect to $m_{t\bar{t}}$ (which scales proportional to $p_{T,t}$ in this configuration), the small change of the top tagging performance due to a change of $p_{T,t}$ is accounted for in our statistical evaluation. Moreover, the tagger we chose to reconstruct the top quarks (HEPTOPTAGGER) is very insensitive against additional radiation, as shown in Ref. [38].

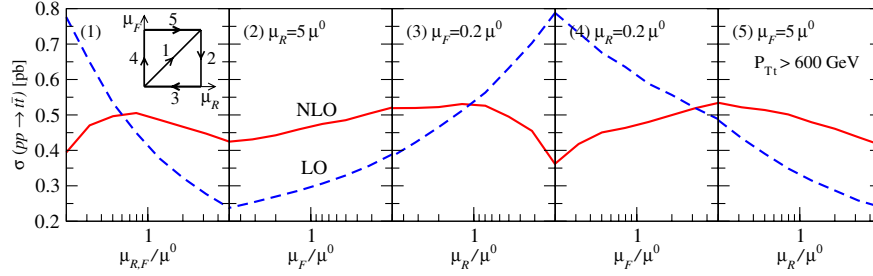


FIG. 3 (color online). Renormalization and factorization scale dependencies for top pair production in the boosted top regime, $p_{T,t} > 600$ GeV. The plot traces the contour in the $\mu_F - \mu_R$ plane with $\mu = (0.2-5)\mu^0$ as shown in the first panel, with μ^0 defined as the event's transverse mass. The results are generated with aMC@NLO for the LHC at $\sqrt{s} = 14$ TeV.

is also still large enough \mathcal{O} (pb) to perform measurements with small statistical uncertainties; the eventual value of $p_{T,\text{fatjet}}$ by the experiments will optimize the systematic uncertainty. This fat jet is then further processed by the HEPTOPTAGGER [36]. Initially the HEPTOPTAGGER was designed to reconstruct only mildly boosted top quarks ($p_{T,t} \approx m_t$) using a very large fat jet cone size. However, in searches for heavy resonances [49] it was shown that due to its flexible reconstruction algorithm and jet grooming procedures the HEPTOPTAGGER is an effective tool for reconstructing highly boosted top quarks while maintaining a small background fake rate. Other top taggers, designed to tag highly boosted top quarks, can be similarly effective [29,50].

After a successful tag, the corresponding jet is removed from the event and we proceed by reclustering the remaining hadronic activity as usual, i.e. by applying the Cambridge/Aachen algorithm with $R = 0.5$. Jets are selected with properties $p_{T,j} > 30$ GeV and $|\eta_j| < 4$. We also require an isolated lepton in the final state with $p_{T,\ell} > 20$ GeV and $|\eta_\ell| < 2.5$ where the lepton is defined as isolated if the transverse energy deposit $E_{T,\text{had}}$ inside a cone around the lepton of size $R = 0.2$ is less than 20% of its transverse energy $E_{T,\ell}$.

On the one hand, the small theoretical uncertainties on the $t\bar{t}$ invariant mass motivates this observable as a suitable choice to examine our BSM hypotheses [28]. From Eq. (5) it becomes clear that dominant BSM corrections are directly reflected in the $m_{t\bar{t}}$ distributions (it is also the variable which typically enters as the only kinematical parameter in total cross section and resummation calculations; see [28,46]). On the other hand, the transverse fat jet momentum and lepton pseudorapidity y_ℓ determine the $t\bar{t}$ + jets kinematics to a large extent for boosted final states. From a boosted top reconstruction point of view, $p_{T,\text{fatjet}}$ is the crucial observable as the threshold largely determines the working point. Since we choose a specific value for $p_{T,\text{fatjet}}$ in our analysis, we turn to $m_{t\bar{t}}$ and y_ℓ in the following.

Missing energy of the final state from the leptonic top decay is not a drawback: the final state neutrino momentum can be reconstructed by requiring transverse momentum conservation and by imposing that the invariant mass

ℓ^\pm -neutrino is equal to m_W . These conditions define, respectively, the neutrino transverse and longitudinal momentum components. To suppress the combinatorics in the $t\bar{t}$ mass reconstruction we need to identify which jet is the most likely to be the b jet, despite not using b tagging in this analysis. This can efficiently be done by identifying the b jet as the closest jet to the lepton with an invariant bottom-lepton mass that satisfies the top decay kinematics [51]

$$m_{b\ell} < \sqrt{m_t^2 - m_W^2} \approx 154.6 \text{ GeV}. \quad (6)$$

After these steps we end up with distributions as depicted in Fig. 4; the BSM-induced shape modification includes a lot of information that we would like to exploit in a binned hypothesis test based on sampling the log-likelihood

$$\mathcal{Q} = -2 \sum_{i \in \text{bins}} n_i^{\text{pseudo}} \log \left(1 + \frac{n_i^{\text{BSM}}}{n_i^{\text{SM}}} \right) - \text{const} \quad (7)$$

with Monte Carlo pseudodata $\{n_i^{\text{pseudo}}\}$, given the input of the (B)SM histograms $\{n_i^{(\text{B})\text{SM}}\}$ [30,52].

There is a caveat. The uncertainties, especially in the $m_{t\bar{t}}$ tails of the distributions, can be large and are currently driven by experimental systematics [39] rather than theoretical limitations (for a recent high precision calculation see [28]). To get a feeling of the size of the systematics we include the relative systematic uncertainty from [39] for $\sqrt{s} = 7$ TeV extrapolated to 14 TeV (see Fig. 4); the theoretical uncertainty of [28] is negligible compared to the systematics of [39]. We map the integrated $m_{t\bar{t}}$ uncertainty to a flat y_ℓ uncertainty; for central tops at transverse momenta of the order of 600 GeV this is a reasonable approximation. It becomes immediately clear that the shape uncertainty will be the limiting factor of this analysis, especially if we want to push limits $R_t, k_V, k_A \rightarrow 0$.

The standard way of including such an uncertainty is via nuisance parameters of the null hypothesis (SM $t\bar{t}$ + jets production in our case) [30,52,53]. When computing the confidence level, these nuisance parameters are marginalized or profiled. However, it can happen that the process

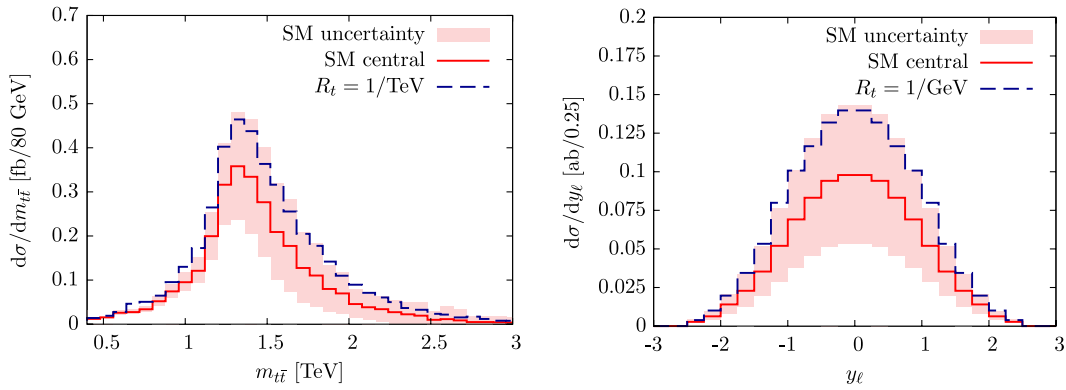


FIG. 4 (color online). Central value and uncertainty distributions of $m_{t\bar{t}}$ and y_ℓ . We also include an exemplary value of $R_t = 1/\text{TeV}$ for comparisons. The uncertainties are based on extrapolating the current 7 TeV uncertainties of Ref. [39] to 14 TeV.

of marginalization hide the systematic uncertainty entirely. By, e.g., including a shape uncertainty to only the null hypothesis and not to the alternative hypothesis, marginalization will shift the median of the toy-sampled log-likelihood distribution for the null hypothesis away from the alternative hypothesis' median. The exclusion in this case appears to be larger than it should be, especially when the uncertainty bands overlap with the difference of null and alternative hypotheses. To avoid issues of this type we include *only* bins which exceed the SM uncertainty to the log-likelihood; i.e. our null hypothesis is the one sigma upwards fluctuated SM hypothesis. This way we reflect the systematic uncertainty in an extremely conservative way; profiling or marginalization will correctly reduce the uncertainty when correlations with other signal regions (e.g. total cross sections and subsidiary top measurements using the ABCD method) are taken into account. This information which requires access to the LHC data samples is not available to us and is also somewhat beyond the scope of this work. We remind the reader to keep in mind that the outlined analysis when performed by the experiments is likely to yield improved constraints eventually.

From Eq. (7) it is clear that the binned log-likelihood approach will pick up sensitivity from regions in the single-valued discriminant where $n_i^{\text{BSM}}/n_i^{\text{SM}}$ is large but still resolvable according to our definition. Hence, the sensitivity is dominated by the p_T threshold behavior of the $t\bar{t}$ sample and jet radiation. There the uncertainty is comparably low $\sim 20\%$ and the *absolute* cross section modification large (keep in mind that the tails of the parton-level distribution grow according to Eq. (5), which does not include the pdf suppression, which quickly limits the considered analysis statistically).

We show the expected 95% exclusion as a function of the integrated luminosity \mathcal{L} in Fig. 5 for three different samples that can be excluded with a data sample of 100/fb at a 14 TeV LHC. The width of the 1 and 2 sigma bands being rather large indicates that we are very close to the border of the discriminable parameter region (in terms of our definition laid out in the previous section). Indeed, for smaller individual values R_t, k_V we cannot formulate constraints as the BSM distribution is entirely covered by the SM uncertainty band. We therefore conclude that an improvement beyond the shown parameter choices depends

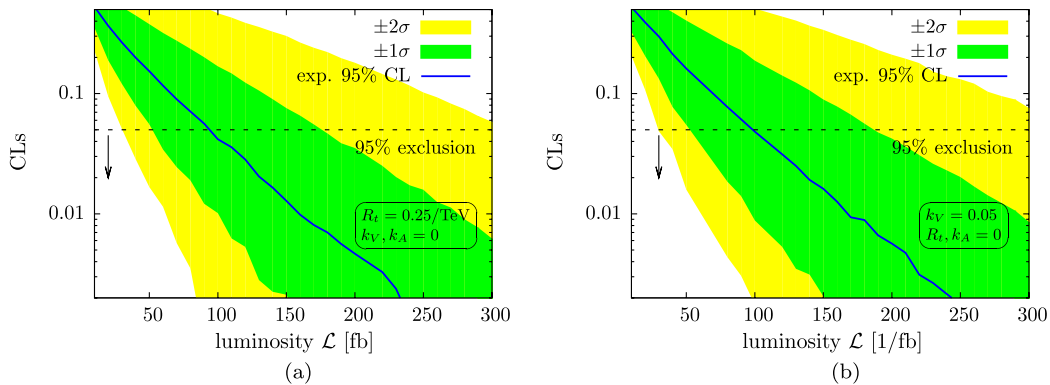


FIG. 5 (color online). Confidence level contours for the operator Eq. (1) in a boosted analysis of $pp \rightarrow t\bar{t} + \text{jets}$ for 14 TeV collisions as described in the text. We pick values of R_t, k_V that can be constrained at luminosities of around 100/fb close to the systematics' threshold.

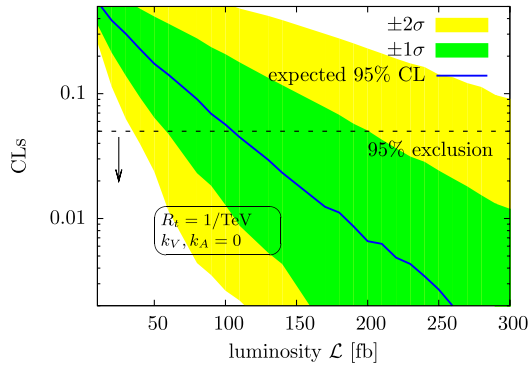


FIG. 6 (color online). Confidence level contours for the operator Eq. (1a) in a boosted analysis of $pp \rightarrow t\bar{t} + \text{jets}$ for 14 TeV collisions as described in the text for a value of $R_t = 1/\text{TeV}$ based on y_ℓ . Choosing $m_{t\bar{t}}$ as the discriminant results in a factor of ~ 4 improvement of the limit setting, Fig. 5.

crucially on the reduction of the experimental systematics (which should be possible when larger data samples are available). As expected the constraints from using $m_{t\bar{t}}$ as a single discriminant are superior to integrated sensitivity observables such as y_ℓ , Fig. 6. For symmetrized uncertainties the above results directly generalize to negative values of the coefficient k_V ; i.e. Fig. 5 can be understood as functions of k_V . There is, however, a caveat that arises with the limit setting approach based on the CLs method that we pursue in this paper: the CLs method, when the null hypothesis is chosen to be the SM, can only constrain cross sections larger than the null hypothesis. To continue our results to negative values we therefore need to interchange null and alternative hypotheses which amounts to a different interpretation statistically speaking.

Comparing to the preliminary investigations of Ref. [26], we find that statistical algorithms, as applied by the experiments and realistic simulation and analysis approaches, show constraints in roughly the same parameter region: $R_t \lesssim 0.25/\text{TeV}$ and $k_V \lesssim 0.05$ at 95% CL. An extrapolation into the $(R_t, k_V, k_A = 0)$ plane is shown in Fig. 7. Since we include differential shape information of the top spectrum and a lower p_T threshold that guarantees a quick saturation of the statistical uncertainty at comparably small luminosities, we obtain more stringent expected constraints than simple correlations of inclusive and exclusive measurements, even when the systematic uncertainty is larger. Working in a consistent expansion to $\sim \Lambda^{-2}$, we can only obtain unrealistically large values on $k_A \gg 1$ that feed into our results through higher jet multiplicities exclusively. The sensitivity on k_A can therefore be rephrased in terms of the additional sensitivity introduced by the extra jet radiation to order $\mathcal{O}(\Lambda^{-2})$: In agreement with Ref. [26] we observe that the impact of the jet matching is a subdominant effect and our sensitivity almost entirely follows from Eq. (5).

We finally comment on the impact of the consistent treatment of the differential cross section to order $\sim \Lambda^{-2}$. In

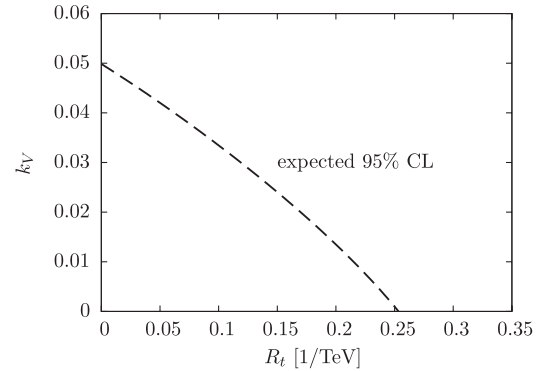


FIG. 7. Confidence level contour for operator Eq. (1) in a boosted analysis of $pp \rightarrow t\bar{t} + \text{jets}$ for 14 TeV collisions as a function of R_t , k_V , $k_A = 0$.

the tails of the distribution it can be expected that terms of order $\sim \Lambda^{-n}$, $n > 2$ become relevant when we resolve the new physics scale. Our quoted limits directly reflect this truncation which is imposed by applying effective field theory to order Λ^{-2} . Some authors, e.g. those of Ref. [54], include Λ^{-4} that arises from the amplitude squared of the new physics contribution. Limits obtained in this way, however, are sensitive to the higher order terms in the same way; i.e., in the phase space region where the limits are driven by Λ^{-4} it can be expected that the dimension eight terms of the Lagrangian have a similar impact on the expected limits. Our limits, therefore, need to be understood with this grain of salt; nonetheless, it is still theoretically consistent with applying effective field theory to Λ^{-2} and statistically consistent with formulating exclusion limits based on CLs. Going beyond the $\sim \Lambda^{-2}$ approximation will be unavoidable if an excess in the tail will be observed.

IV. CONCLUSIONS AND OUTLOOK

The discovery of a Higgs boson that seems to follow the SM paradigm and the lack of any hints toward natural physics completions at the TeV scale prompts us to study the heavy degrees of freedom of the SM more carefully. Top quark physics, typically considered an impediment for new physics searches by providing a major background contribution, is a well-motivated candidate for such analyses. The abundant production of top pairs at the LHC allows us to tightly constrain the smallest resolvable deviations from the SM-predicted coupling pattern that is expected to be observed if the top quark arises (partially) as a bound state of a strongly interacting sector. This option is widely discussed in the literature, and investigating anomalous QCD interactions in the top sector provides a path to either observe or strongly constrain such a scenario.

Resolving a potential composite structure with large momentum transfers in the top sector naturally motivates

boosted top analyses as highly sensitive channels. Reconstruction techniques are under good theoretical control and have successfully been applied in $t\bar{t}$ resonance searches [39]. Such resonances are expected in strongly interacting theories, too, but typical composite interactions can be expected to predominantly manifest themselves in a large deviation of the $t\bar{t}$ spectrum's tail, and experimental and theoretical uncertainties become major limitations of such searches.

In this paper we have computed the expected 95% confidence level constraints on a set of non-SM effective top QCD interactions resulting from an exemplary boosted top analysis and a representative set of operators. We have included the dominant first hard gluon radiation effects in a matched approach. Systematic differential uncertainties are the key limiting factors of our analysis. We take these into account in the most conservative way and base them on extrapolating current 7 TeV measurements to 14 TeV. We can therefore expect our constraints to be on the conservative end and believe that the actual analysis when performed by the experiments can indeed improve on our results.

Our hadron-level analysis correctly captures the top tagging's varying efficiency as a function of the anomalous parameters. This together with a state-of-the-art binned

log-likelihood formulation of the expected confidence level constraints shows that differential shape information supercedes the naive extrapolation of earlier theoretical work, even when errors are considerably larger. We find that we should be able to probe an anomalous chromomagnetic moment at the percent level and QCD-induced top radii at $\lesssim 0.25/\text{TeV}$.

In summary, the search for a potential top substructure strongly benefits from recent developments in jet substructure analysis techniques. Adapting existing boosted top searches to BSM scenarios of this type is a straightforward exercise in the light of the results of Ref. [39]. Given that this is an alternative route to study theoretically well-motivated scenarios beyond the SM, we hope that this is incentive enough for the experiments to eventually perform measurements as outlined here.

ACKNOWLEDGMENTS

We thank James Ferrando and Olivier Mattelaer for helpful conversations. We also thank Ben Pecjak for providing the results of Ref. [28]. C.E. thanks David Miller, Liam Moore, Michael Russell, and Chris White for discussions on the topic. C.E. is supported in part by the IPPP Associateship programme.

-
- [1] F. Englert and R. Brout, *Phys. Rev. Lett.* **13**, 321 (1964); P. W. Higgs, *Phys. Lett.* **12**, 132 (1964); *Phys. Rev. Lett.* **13**, 508 (1964); G. S. Guralnik, C. R. Hagen, and T. W. B. Kibble, *Phys. Rev. Lett.* **13**, 585 (1964).
- [2] ATLAS Collaboration, *Phys. Lett. B* **716**, 1 (2012).
- [3] CMS Collaboration, *Phys. Lett. B* **716**, 30 (2012).
- [4] ATLAS Collaboration, Report No. ATLAS-CONF-2013-034.
- [5] S. Chatrchyan *et al.* (CMS Collaboration), *J. High Energy Phys.* **06** (2013) 081.
- [6] C. D. Froggatt and H. B. Nielsen, *Nucl. Phys.* **B147**, 277 (1979).
- [7] For a review see, e.g., H. P. Nilles, *Phys. Rep.* **110**, 1 (1984).
- [8] M. Shaposhnikov and C. Wetterich, *Phys. Lett. B* **683**, 196 (2010).
- [9] K. Agashe, R. Contino and A. Pomarol, *Nucl. Phys.* **B719**, 165 (2005).
- [10] R. Contino, Y. Nomura, and A. Pomarol, *Nucl. Phys.* **B671**, 148 (2003); K. Agashe, R. Contino, and A. Pomarol, *Nucl. Phys.* **B719**, 165 (2005).
- [11] G. F. Giudice, C. Grojean, A. Pomarol, and R. Rattazzi, *J. High Energy Phys.* **06** (2007) 045.
- [12] A. Pomarol and J. Serra, *Phys. Rev. D* **78**, 074026 (2008).
- [13] R. Contino, M. Ghezzi, C. Grojean, M. Muhlleitner, and M. Spira, *J. High Energy Phys.* **07** (2013) 035; A. Alloul, B. Fuks, and V. Sanz, [arXiv:1310.5150](https://arxiv.org/abs/1310.5150).
- [14] B. R. Holstein, *Nucl. Phys.* **A689**, 135 (2001).
- [15] H. Geiger and E. Marsden, *Proc. R. Soc. A* **82**, 495 (1909).
- [16] E. Rutherford, *Philos. Mag.* **21**, 669 (1911).
- [17] H. Geiger, E. Marsden, and E. Rutherford, *Philos. Mag.* **25**, 604 (1913).
- [18] H. Georgi, L. Kaplan, D. Morin, and A. Schenk, *Phys. Rev. D* **51**, 3888 (1995).
- [19] K.-I. Hikasa, K. Whisnant, J. M. Yang, and B.-L. Young, *Phys. Rev. D* **58**, 114003 (1998).
- [20] W. Buchmüller and D. Wyler, *Nucl. Phys.* **B268**, 621 (1986).
- [21] B. Grzadkowski, M. Iskrzynski, M. Misiak, and J. Rosiek, *J. High Energy Phys.* **10** (2010) 085.
- [22] C. Degrande, J.-M. Gerard, C. Grojean, F. Maltoni, and G. Servant, *J. High Energy Phys.* **03** (2011) 125; C. Degrande, [arXiv:1207.5069](https://arxiv.org/abs/1207.5069).
- [23] J. A. Aguilar-Saavedra, *Nucl. Phys.* **B812**, 181 (2009).
- [24] P. Haberl, O. Nachtmann, and A. Wilch, *Phys. Rev. D* **53**, 4875 (1996).
- [25] D. Atwood, A. Kagan, and T. G. Rizzo, *Phys. Rev. D* **52**, 6264 (1995); K. M. Cheung, *Phys. Rev. D* **55**, 4430 (1997); B. Lillie, J. Shu, and T. M. P. Tait, *J. High Energy Phys.* **04** (2008) 087; K. Kumar, T. M. P. Tait, and R. Vega-Morales, *J. High Energy Phys.* **05** (2009) 022; Z. Hioki and K. Ohkuma, *Eur. Phys. J. C* **65**, 127 (2010); D. Choudhury and P. Saha, *Pramana* **77**, 1079 (2011); Z. Hioki and

- K. Ohkuma, *Phys. Lett. B* **716**, 310 (2012); H. Hesari and M. M. Najafabadi, [arXiv:1207.0339](https://arxiv.org/abs/1207.0339); M. Baumgart and B. Tweedie, *J. High Energy Phys.* **03** (2013) 117; A. Hayreter and G. Valencia, *Phys. Rev. D* **88**, 034033 (2013); E. Gabrielli and M. Raidal, *Phys. Rev. D* **84**, 054017 (2011); E. Gabrielli, M. Raidal, and A. Racioppi, *Phys. Rev. D* **85**, 074021 (2012).
- [26] C. Englert, A. Freitas, M. Spira, and P. M. Zerwas, *Phys. Lett. B* **721**, 261 (2013).
- [27] A. Abdesselam *et al.*, *Eur. Phys. J. C* **71**, 1661 (2011); A. Altheimer *et al.*, *J. Phys. G* **39**, 063001 (2012); T. Plehn and M. Spannowsky, *J. Phys. G* **39**, 083001 (2012).
- [28] A. Ferroglia, B. D. Pecjak, and L. L. Yang, *J. High Energy Phys.* **09** (2013) 032.
- [29] D. E. Soper and M. Spannowsky, *Phys. Rev. D* **87**, 054012 (2013).
- [30] A. L. Read, Report No. CERN-OPEN-2000-205; A. L. Read, *J. Phys. G* **28**, 2693 (2002); G. Cowan, K. Cranmer, E. Gross, and O. Vitells, *Eur. Phys. J. C* **71**, 1554 (2011).
- [31] S. J. Brodsky and S. D. Drell, *Phys. Rev. D* **22**, 2236 (1980).
- [32] J. S. Schwinger, *Phys. Rev.* **73**, 416 (1948); J. Jersak, E. Laermann, and P. M. Zerwas, *Phys. Rev. D* **25**, 1218 (1982); **36**, 310 (1987).
- [33] E. Boos, L. Dudko, and T. Ohl, *Eur. Phys. J. C* **11**, 473 (1999); F. Bach and T. Ohl, *Phys. Rev. D* **86**, 114026 (2012).
- [34] Y. Grossman and M. Neubert, *Phys. Lett. B* **474**, 361 (2000); S. J. Huber and Q. Shafi, *Phys. Lett. B* **498**, 256 (2001).
- [35] J. L. Hewett, J. Shelton, M. Spannowsky, T. M. P. Tait, and M. Takeuchi, *Phys. Rev. D* **84**, 054005 (2011).
- [36] T. Plehn, G. P. Salam, and M. Spannowsky, *Phys. Rev. Lett.* **104**, 111801 (2010); T. Plehn, M. Spannowsky, M. Takeuchi, and D. Zerwas, *J. High Energy Phys.* **10** (2010) 078.
- [37] J. Alwall, S. de Visscher, and F. Maltoni, *J. High Energy Phys.* **02** (2009) 017.
- [38] K. Joshi, A. D. Pilkington, and M. Spannowsky, *Phys. Rev. D* **86**, 114016 (2012).
- [39] G. Aad *et al.* (ATLAS Collaboration), *J. High Energy Phys.* **09** (2012) 041.
- [40] ATLAS Collaboration, Report No. ATLAS-CONF-2013-052.
- [41] N. D. Christensen and C. Duhr, *Comput. Phys. Commun.* **180**, 1614 (2009).
- [42] C. Degrande, C. Duhr, B. Fuks, D. Grellscheid, O. Mattelaer, and T. Reiter, *Comput. Phys. Commun.* **183**, 1201 (2012); P. de Aquino, W. Link, F. Maltoni, O. Mattelaer, and T. Stelzer, *Comput. Phys. Commun.* **183**, 2254 (2012).
- [43] J. Alwall, M. Herquet, F. Maltoni, O. Mattelaer, and T. Stelzer, *J. High Energy Phys.* **06** (2011) 128.
- [44] T. Sjostrand, L. Lonnblad, S. Mrenna, and P. Z. Skands, [arXiv:hep-ph/0308153](https://arxiv.org/abs/hep-ph/0308153).
- [45] M. L. Mangano, M. Moretti, F. Piccinini, and M. Treccani, *J. High Energy Phys.* **01** (2007) 013.
- [46] S. Moch and P. Uwer, *Phys. Rev. D* **78**, 034003 (2008); M. Czakon, P. Fiedler, and A. Mitov, *Phys. Rev. Lett.* **110**, 252004 (2013).
- [47] V. Hirschi, R. Frederix, S. Frixione, M. V. Garzelli, F. Maltoni, and R. Pittau, *J. High Energy Phys.* **05** (2011) 044; R. Frederix and S. Frixione, *J. High Energy Phys.* **12** (2012) 061; P. Torrielli and S. Frixione, *J. High Energy Phys.* **04** (2010) 110.
- [48] M. Cacciari, G. P. Salam, and G. Soyez, *Eur. Phys. J. C* **72**, 1896 (2012).
- [49] G. Aad *et al.* (ATLAS Collaboration), *J. High Energy Phys.* **01** (2013) 116; G. Aad *et al.* (ATLAS Collaboration), *J. High Energy Phys.* **09** (2013) 076; ATLAS Collaboration, Report No. ATLAS-CONF-2013-084.
- [50] D. E. Kaplan, K. Rehermann, M. D. Schwartz, and B. Tweedie, *Phys. Rev. Lett.* **101**, 142001 (2008); L. G. Almeida, S. J. Lee, G. Perez, I. Sung, and J. Virzi, *Phys. Rev. D* **79**, 074012 (2009); M. Jankowiak and A. J. Larkoski, *J. High Energy Phys.* **06** (2011) 057; J. Thaler and K. Van Tilburg, *J. High Energy Phys.* **02** (2012) 093; M. Backovic and J. Juknevich, *Comput. Phys. Commun.* **185**, 1322 (2014); S. Schaetzel and M. Spannowsky, *Phys. Rev. D* **89**, 014007 (2014).
- [51] T. Plehn, M. Spannowsky, and M. Takeuchi, *J. High Energy Phys.* **05** (2011) 135.
- [52] T. Junk, *Nucl. Instrum. Methods Phys. Res., Sect. A* **434**, 435 (1999); T. Junk, CDF Note 8128 [[cdf/doc/statistics/public/8128](https://arxiv.org/abs/cdf/doc/statistics/public/8128)]; T. Junk, CDF Note 7904 [[cdf/doc/statistics/public/7904](https://arxiv.org/abs/cdf/doc/statistics/public/7904)]; H. Hu and J. Nielsen, Report No. CERN 2000-005, 2000.
- [53] G. Cowan, K. Cranmer, E. Gross, and O. Vitells, *Eur. Phys. J. C* **71**, 1554 (2011).
- [54] J. F. Kamenik, M. Papucci, and A. Weiler, *Phys. Rev. D* **85**, 071501 (2012).